AIR MINISTRY.

(T. 2553 & A.)

AERONAUTICAL RESEARCH COMMITTEE.

REPORTS AND MEMORANDA No. 1176.
(Ae. 340.)

THE BOUNDARY LAYER OF THE FRONT PORTION OF A CYLINDER.

By A. Thom, B.Sc., Ph.D.

Communicated by Professor J. D. Cormack.

JULY, 1928.

LONDON:
PRINTED AND PUBLISHED BY HIS MAJESTY'S STATIONERY OFFICE
To be purchased directly from H.M. STATIONERY OFFICE at the following addresses:
Adastral House, Kingsway, London, W.C.2; 120, George Street, Edinburgh;
York Street, Manchester; 1, St. Andrew's Crescent, Cardiff;
15, Donegall Square West, Belfast;
or through any Bookseller.

1928

Price 1s. 0d. Net.

23-9999.

AERODYNAMIC SYMBOLS

1. GENERAL

m mass

t time

V resultant linear velocity

Ω resultant angular velocity

ρ density, σ relative density

ν kinematic coefficient of viscosity

R Reynolds number, $R = lV/\nu$ (where l is a suitable linear dimension), to be expressed as a numerical coefficient $\times 10^6$

Normal temperature and pressure for aeronautical work are 15° C. and 760 mm.

For air under these conditions $\begin{cases} \rho = 0{\cdot}002378 \text{ slug/cu. ft.} \\ \nu = 1{\cdot}59 \times 10^{-4} \text{ sq. ft./sec.} \end{cases}$

The slug is taken to be 32·2 lb.-mass.

α angle of incidence

ϵ angle of downwash

S area

c chord

s semi-span

A aspect ratio, $A = 4s^2/S$

L lift, with coefficient $k_L = L/S\rho V^2$

D drag, with coefficient $k_D = D/S\rho V^2$

γ gliding angle, $\tan\gamma = D/L$

L rolling moment, with coefficient $k_l = L/sS\rho V^2$

M pitching moment, with coefficient $k_m = M/cS\rho V^2$

N yawing moment, with coefficient $k_n = N/sS\rho V^2$

2. AIRSCREWS

n revolutions per second

D diameter

J V/nD

P power

T thrust, with coeffic

Q torque, with coeffici

η efficiency, $\eta = TV/P$

THE BOUNDARY LAYER OF THE FRONT PORTION OF A CYLINDER.

By A. Thom, B.Sc., Ph.D.

Communicated by Professor J. D. Cormack.

Reports and Memoranda No. 1176.
(Ae. 340.)

July, 1928.

Introduction.—A large amount of information is now available regarding the flow of water or air past a cylinder placed across the stream so far as the behaviour of the main body of the fluid is concerned; but the conditions in the layer close to the surface of the cylinder seem to be largely unknown. Accordingly it seemed advisable to explore the velocity, etc., close to the surface. This paper consists of two parts, first, a description of experiments on the boundary layer carried out in the Summer of 1927 in the James Watt Engineering Laboratories, University of Glasgow, and second, a theory of the boundary layer over the front portion of the cylinder based on Prandtl's simplified boundary layer equations as given by Bairstow in his illuminating paper on Skin Friction to the Royal Aeronautical Society in January, 1925.

Experiments.—The cylinder used for these experiments was of brass 4·5 inches in diameter, turned and ground true. The resulting surface was smooth but was not polished. The cylinder extended across the wind channel which is approximately 2 ft. square. As it is the boundary layer which is under consideration the relative largeness of the cylinder compared to the channel dimensions can hardly affect the results. Since the boundary layer theory assumes a knowledge of the pressures and velocities outside the skin the pressure distribution was first obtained by drilling a small hole in the central section of the cylinder. As the cylinder could be rotated to any position a comparison of the pressure in this hole with that in a similar hole in a plate on the channel wall, for various positions of the hole, gave the required pressure distribution. This was done for channel speeds of 12·3 and 36 ft./sec.

The results are given in Table 2 and shown plotted in fig. 1. No corrections have been applied to these figures and subsequent experiment showed that they are referred to a pressure which is

$0 \cdot 02\ \rho V^2$ below the undisturbed static pressure in the channel. The values given for k_D at the foot of Table 2 were obtained by integrating the drag component of the pressure round the cylinder.

A small static tube about 0·6 mm. diameter was used to test the constancy of the static pressure through the boundary layer. As was to be expected the results showed that the static pressure over distances of the order of 1 or 2 mm. is practically constant and equal to the pressure on the surface at the point considered. This simplifies the measurement of velocity as it is now only necessary to measure the total head at a point near the surface to obtain the velocity, the static head being taken from the distribution of pressure as given on fig. 1.

The method used to measure the total head was as follows :—

A small open-ended or Pitot tube was mounted on a micrometer arrangement so that the end of the tube could be traversed along the normal. Provision was made for mounting the arrangement in any position round the cylinder. The pressures were measured on an ordinary tilting gauge manometer detecting pressure changes of about 0·0003 inches of water. The Pitot tubes were made by drawing a glass tube down to a diameter of about $1\frac{1}{2}$ mm., and then drawing a section of this down to the required diameter. The tube was then broken off and the ends ground square on a fine stone. As the diameters used varied from about 0·23 mm. upwards, this was a delicate operation.

It was found desirable to fill the tube with wax before attempting to grind the end, thus preventing the bore becoming choked with chips, etc., which cannot afterwards be removed. A great many of these tubes were made and tested. It was found that if the bore was less than about 0·1 mm., the damping effect produced was so great that the tube was practically useless when used in conjunction with the usual tilting manometer. With care, the wall thickness can be controlled and made about 0·05 mm., so that the overall diameter has a lower limit of about 0·2 mm. If the tube is made oval a slight advantage is gained as the centre can then be brought slightly nearer the surface for a given area of bore. The most useful tube of all those made, measured $0 \cdot 36 \times 0 \cdot 45$ mm. externally. This permitted the velocity to be measured at 0·18 mm. from the surface.

It was necessary to find if these small tubes gave an accurate measure of total head. This point has already been investigated by Miss M. Barker (Mrs. Glauert)* using a small pitot in water but it was considered advisable to test the actual tubes being used in air. Accordingly, a number were compared at various velocities

*Proc. Roy. Soc. A.101.

with a larger pitot tube about 5 mm. diameter. It was found that at low velocities the smaller tubes tended to give higher pressures than the large tube.

Let H = pressure in small pitot tube.
p = the static pressure at the point and
d = tube diameter.

Then $H - p = f(vd/\nu)\ \rho v^2$

The large tube is assumed to give a pressure of $\frac{1}{2}\rho v^2$ above static pressure. Hence if the tubes are connected to opposite sides of the manometer the latter will read $H - p - \frac{1}{2}\rho v^2$ or

$$\rho v^2 \left\{ f(v\,d/\nu) - \frac{1}{2} \right\} \text{ so we get}$$

$$f(v\,d/\nu) - \frac{1}{2} = (\text{Manometer reading}) \div \rho v^2$$

It is only at low values of vd/ν that $f(vd/\nu)$ will differ from $\frac{1}{2}$. It is difficult to get this low vd because reducing v reduces the pressures being dealt with and reducing d introduces the damping trouble already mentioned, so that no great accuracy is possible in the determination of $f(vd/\nu)$ by this method. About 40 readings were taken with different tubes at various velocities. The individual readings are scattered and uncertain and the mean results as presented in Table 1 are only given to show the corrections applied to the subsequent measurements of total head.

TABLE 1.

Mean vd ft.²/sec.	Mean vd/ν	Mean $f(vd/\nu)$
0·004	25	0·64
0·006	38	0·61
0·009	56	0·58
0·013	81	0·54
0·018	113	0·52
0·025	157	0·50

When a Pitot is placed with its end in a field where the total head is varying rapidly along the normal it may not be correct to assume that the pressure given by the tube corresponds to the total head at the centroid of the end. Involved with this question is that of the effect of the proximity of the surface when the tube is very close to the latter. These points were investigated by exploring the same normal section with tubes of different sizes. (*See* Table 3 and fig. 4, $\theta = 60°$.)

(34641) Wt. 51/6007/1607 375 1/29 Harrow G. 7/1

It appears that the error, if any, due to assuming the pressure in the tube equal to the total head at the position occupied by its centre is smaller than the experimental errors except when the tube is practically touching the surface when it perhaps reads a trifle high.

The total head was measured along the normals at 10 degree intervals from $\theta = 10°$ to $\theta = 90°$ with a channel speed of 12·3 ft./sec. In each case the tube was placed parallel to the surface. In all about 180 measurements were made with tubes varying in diameter from 0·36 to 0·9 mm. The results are given in Table 3, practically all the tabulated values being means of two or more readings. Table 3 also gives additional measurements made at $\theta = 50°$ with wind speeds of 5·4 and 22·5 ft./sec. Where necessary, all these results have been corrected for the scale effect already mentioned (Table 1). In most cases the correction brought the results obtained from different tubes into closer agreement. The figures tabulated for $n = 0$ in each case are taken from the measures of surface pressures (Table 2) since at the surface the static pressure and the total head are equal, the velocity being zero. Table 3 also gives the velocities corresponding to the measured pressures.

Theory.—In the paper already referred to, Bairstow gives the boundary layer equations as

$$q\frac{\partial q}{\partial s} + w\frac{\partial q}{\partial n} = -\frac{1}{\rho}\frac{\partial p}{\partial s} + \nu\frac{\partial^2 q}{\partial n^2} \quad .. \quad (1)$$

$$0 = \frac{1}{\rho}\frac{\partial p}{\partial n} \quad .. \quad .. \quad .. \quad (2)$$

$$\frac{\partial q}{\partial s} + \frac{\partial w}{\partial n} = 0 \quad .. \quad .. \quad .. \quad .. \quad (3)$$

where n and s are measured normal and tangential to the surface, the component velocities being w and q.

The solution thereafter given for a flat plate is based on the fact that $\partial p/\partial s$ can be neglected. In the case of the flow over the surface of a cylinder this assumption is no longer permissible; in fact $\partial p/\partial s$ turns out to be the controlling factor in the solution later presented.

A step by step method of solution was used first as follows :— Let A, B, C and D be four points on the corners of a small rectangle in the boundary layer and O the centre point

D · · A

· O

C · · B

Let q, w, etc., be the values of the quantities at O, and q_m be the average of q_A, q_B, q_C and q_D.

Then

$$\left.\begin{aligned}
q_A &\doteqdot q + s\frac{\partial q}{\partial s} + \frac{s^2}{2}\frac{\partial^2 q}{\partial s^2} + n\frac{\partial q}{\partial n} + \frac{n^2}{2}\frac{\partial^2 q}{\partial n^2} + n\,s\,\frac{\partial^2 q}{\partial n\,\partial s}\\
q_B &\doteqdot q + s\frac{\partial q}{\partial s} + \frac{s^2}{2}\frac{\partial^2 q}{\partial s^2} - n\frac{\partial q}{\partial n} + \frac{n^2}{2}\frac{\partial^2 q}{\partial n^2} - n\,s\,\frac{\partial^2 q}{\partial n\,\partial s}\\
q_C &\doteqdot q - s\frac{\partial q}{\partial s} + \frac{s^2}{2}\frac{\partial^2 q}{\partial s^2} - n\frac{\partial q}{\partial n} + \frac{n^2}{2}\frac{\partial^2 q}{\partial n^2} + n\,s\,\frac{\partial^2 q}{\partial n\,\partial s}\\
q_D &\doteqdot q - s\frac{\partial q}{\partial s} + \frac{s^2}{2}\frac{\partial^2 q}{\partial s^2} + n\frac{\partial q}{\partial n} + \frac{n^2}{2}\frac{\partial^2 q}{\partial n^2} - n\,s\,\frac{\partial^2 q}{\partial n\,\partial s}
\end{aligned}\right\} \quad (4)$$

where, for the moment, s and n are the co-ordinates of A relative to O. Adding and re-arranging we get

$$q = q_m - \frac{n^2}{2}\left(\frac{\partial^2 q}{\partial n^2} + \frac{s^2}{n^2}\frac{\partial^2 q}{\partial s^2}\right) \quad .. \quad .. \quad (5)$$

We have from (1) a value of $\partial^2 q/\partial n^2$ to substitute in (5). If s^2/n^2 is of the order unity we are justified in neglecting $\partial^2 q/\partial s^2$ since it is neglected in forming (1). By suitable combinations of (4) we obtain the obvious expressions

$$\partial q/\partial s = (q_A + q_B - q_C - q_D) \div 4s$$
$$\partial q/\partial n = (q_A + q_D - q_B - q_C) \div 4n$$

Making these substitutions in (5) it becomes

$$\begin{aligned} q = q_m &- k_1 q\,(q_A + q_B - q_C - q_D)\\ &- k_2 w\,(q_A + q_D - q_B - q_C) + k_3 \end{aligned} \quad .. \quad (6)$$

where

$$k_1 = n^2/8\,\nu\,s,\ k_2 = n^2/8\,\nu\,n,\ k_3 = -\frac{n^2}{2\,\nu\,\rho}\frac{\partial p}{\partial s}$$

If a velocity distribution is assumed throughout the boundary layer and the assumed field divided into rectangles then the velocity q at the centre of each rectangle can be calculated from the assumed values at the corners by means of (6). A second approximation can then be obtained by using the calculated central velocities to compute new " corner " velocities. The process is repeated until identical values are obtained on succeeding repetitions. Strictly speaking the velocity w at each corner should be calculated from (3) at each cycle of operations. For this purpose write (3)

$$d\,w = -(\partial q/\partial s)\,d\,n$$

and integrate graphically or mechanically. In practice the w term had so little effect on (6) (throughout the region tried) that the integration had only to be performed once in several cycles.

The above method was applied to obtain an approximate solution for the front portion of the cylinder. For this purpose the radius was taken as unity (1 ft.) and the channel velocity 100 ft./sec. As VD/ν for the experiment already described was about 28,000, a value of ν was used which would give the same Reynold's number. The intervals used for s correspond to 2 degrees and the n intervals are 0·002. The pressures round the cylinder are shown in fig. 1. For present purposes a good approximation to these values from $\theta = 0$ to $\theta = 35°$ is $p - p_0 = \frac{1}{2}\rho V^2 (1 - 3{\cdot}5 \sin^2 \theta)$ against $p - p_0 = \frac{1}{2}\rho V^2 (1 - 4 \sin^2 \theta)$ for a perfect fluid. Then, the velocity outside the boundary layer is

$$v = \sqrt{3{\cdot}5}\ V \sin\ \theta, \text{ and } \frac{1}{\rho}\frac{\partial p}{\partial s} = -\frac{V^2}{r}\, 3{\cdot}5 \sin\ \theta \cos\ \theta.$$

It follows that

$$k_1 = 1/500,\ k_2 = 1/28{\cdot}6,\ k_3 = 999 \sin\ \theta \cos\ \theta.$$

A start was made by assuming that on the surface $q = 0$, and at $n = 0{\cdot}008$, $q = v$.

Many cycles were calculated, the last two being shown in Table 4 up to $\theta = 20°$. The upper figures in the squares at $\theta = 4°, 8°, 12°$, etc., are assumed values of q obtained from previous trials. Values of $k_2 w$ at $\theta = 0$ and $\theta = 20°$ as obtained by graphical integrations are given in the outer columns. From these figures the values of q at $\theta = 2°, 6°$, etc., were computed and then from these the lower values in the other squares were obtained. The agreement with the assumed values indicates that the process has been carried far enough. The solution was not extended far round the cylinder since a new method of attack suggested itself as a result of an examination of the figures obtained in the first 20 degrees.

It will be noticed that q/v at any definite value of n is nearly independent of θ., i.e., of s.

Assume then as a first approximation that we can write $q = vx$ where v is the velocity outside the boundary layer and x is a function of n only. Also in the first approximation neglect the term $w\partial q/\partial n$. (Corrections are made at a later stage for the errors introduced by these assumptions.)

Then we have

$$\left.\begin{aligned} q = v\,x,\ \partial q/\partial n = v\,\partial x/\partial n, \\ \partial^2 q/\partial n^2 = v\,d^2 x/d n^2,\ \partial q/\partial s = x\,d v/d s \end{aligned}\right\} \quad \ldots \quad (7)$$

We also have

$$p + \frac{1}{2}\rho v^2 = p_0 + \frac{1}{2}\rho V^2 \quad .. \quad .. \quad (8)$$

where V = channel speed, which on differentiation yields

$$\frac{dv}{ds} = -\frac{1}{\rho\nu}\frac{dp}{ds} \quad .. \quad .. \quad .. \quad (9)$$

Substituting these values in (1) and dividing by v we get

$$\frac{dv}{ds}x^2 - \frac{dv}{ds} = \nu\frac{d^2x}{dn^2} \quad .. \quad .. \quad (10)$$

Multiply through by 2 dx/dn and integrate obtaining

$$\frac{2}{3}\frac{dv}{ds}x^3 - 2\frac{dv}{ds}x = \nu\left(\frac{dx}{dn}\right)^2 + C \quad .. \quad .. \quad (11)$$

When

$$x = 1,\ dx/dn = 0 \text{ giving } C = -\frac{4}{3}\frac{dv}{ds}$$

Hence,

$$\frac{dn}{dx} = \sqrt{\left(\frac{3\nu}{2\,dv/ds}\right)} \div \sqrt{(x^3 - 3x + 2)} \quad .. \quad (12)$$

or

$$n = \sqrt{\left(\frac{3\nu}{2\,dv/ds}\right)}\int \frac{dx}{(1-x)\sqrt{(x+2)}} \quad .. \quad (13)$$

Performing the integration and noting that when $n = 0$, $x = 0$ gives

$$n = \sqrt{\left(\frac{3\nu}{2\,dv/ds}\right)} \cdot \frac{2}{\sqrt{3}} \log \frac{(\sqrt{3}-\sqrt{2})\sqrt{(1-x)}}{\sqrt{3}-\sqrt{(x+2)}} \quad .. \quad (14)$$

This can be compared with the previous mechanical solution directly, but it is perhaps better to put it in a form with the dimensional and non-dimensional parts separated as follows :

Put

$$p_1 = (p - p_0) \div \frac{1}{2}\rho V^2$$

then we have from (8)

$$v = V\sqrt{1 - p_1} \quad .. \quad .. \quad .. \quad (15)$$

so that dv/ds can be written

$$\frac{dv}{ds} = -\frac{1}{\rho v}\frac{dp}{ds} = \frac{-V}{2\sqrt{(1-p_1)}}\frac{dp_1}{ds}$$
$$= \frac{-V}{2r\sqrt{(1-p_1)}}\frac{dp_1}{d\theta} = \frac{V\,h}{r}$$

where r = radius of cylinder and

$$h = \frac{-1}{2\sqrt{(1-p_1)}}\frac{dp_1}{d\theta} \quad .. \quad .. \quad (16)$$

Hence (14) becomes

$$n = \sqrt{\left(\frac{r\nu}{V\,h}\right)} \cdot \sqrt{2}\log\frac{(\sqrt{3}-\sqrt{2})\sqrt{(1-x)}}{\sqrt{3}-\sqrt{(x+2)}} \quad .. \quad (17)$$

For comparison with forms to be developed later it is convenient to write this

$$n = \sqrt{\left(\frac{r\nu}{V\,h}\right)}\,F(x) \quad .. \quad .. \quad .. \quad (18)$$

The advantage of using h instead of dv/ds is that for a given value of θ, h is constant and independent of VD/ν so long as the pressure curve (fig. 1) is unaltered.

A comparison of theory and experiment is given in fig. 3.

The experimental values of Table 3 have been reduced by putting $x = q/v$ and $F(x) = n\sqrt{(Vh/r\nu)}$, v and h being the appropriate values for the section as given by (15) and (16). (*See* Table 5.)

The full line represents the above approximate solution, that is

$$F(x) = \sqrt{2}\log\frac{(\sqrt{3}-\sqrt{2})\sqrt{(1-x)}}{\sqrt{3}-\sqrt{(x+2)}}$$

while the values obtained by the mechanical method (Table 4) are shown by arrows. It is evident that the mechanical solution gives better agreement with the observed values than (17). This is only to be expected considering the assumptions made in deducing (17).

A brief examination will now be made of the terms neglected in the previous theory, using where necessary the results of the first approximation.

The Term $w\,\partial q/\partial n$:—From (3) and (7) we have

$$w = -\int\frac{dq}{ds}\,dn \doteqdot -\frac{dv}{ds}\int x\,dn \text{ and } \frac{\partial q}{\partial n} = v\frac{dx}{dn}$$

Re-writing (12) as

$$\frac{d\,n}{d\,x} = \sqrt{\left(\frac{r\,\nu}{\mathrm{V}h}\right)}\,\mathrm{F}'\,(x)$$

where

$$\mathrm{F}'\,(x) = \sqrt{\frac{3}{2\,(x^3 - 3\,x + 2)}}$$

and substituting these values leads to

$$w\,\frac{\partial\,q}{\partial\,n} \doteqdot -\,v\,\frac{d\,v}{d\,s}\,\frac{1}{\mathrm{F}'\,(x)}\int x\,\mathrm{F}'\,(x)\,d\,x = (\text{say}) - v\,\frac{d\,v}{d\,s}\,\varphi\,(x)$$

where

$$\varphi\,(x) = \int x\,\mathrm{F}'\,(x)\,d\,x \div \mathrm{F}'\,(x)$$

Retaining this value of $w\,\partial\,q/\partial\,n$ in (1), equation (10) becomes

$$\frac{d\,v}{d\,s}\,x^2 - \frac{d\,v}{d\,s}\,\varphi\,(x) - \frac{d\,v}{d\,s} = \nu\,\frac{d^2\,x}{d\,n^2}$$

Treating this as (10) was previously treated yields

$$\frac{d\,n}{d\,x} = \sqrt{\left(\frac{3\,\nu}{2\,d\,v/d\,s}\right)} \div \sqrt{\left\{x^3 - 3\,x + 2 + 3\int_{x\,=\,x}^{x\,=\,1} \varphi\,(x)\,d\,x\right\}} \quad (19)$$

The integral in (19) is easily evaluated graphically or by mechanical quadrature and once done it applies to all sections. This has come about because $w\,\partial\,q/\partial\,n$ is linear with $\partial\,v/\partial\,s$ (*see* above). In the term to be dealt with next, this does not hold necessitating a separate integration for every section.

The Term $\partial\,x/\partial\,s$:—In the analytical solution above it was assumed that $\partial\,q/\partial\,s$ was equal to $x\,d\,v/d\,s$. This can only be regarded as a crude approximation. We shall now write :—

$$\frac{\partial\,q}{\partial\,s} = x\left(\frac{d\,v}{d\,s}\right)_n + v\left(\frac{d\,x}{d\,s}\right)_n$$

the subscript indicating the variable to be considered constant. Considering n as a function of s and x we have

$$\left(\frac{d\,x}{d\,s}\right)_n = -\,\frac{\left(\frac{d\,n}{d\,s}\right)_x}{\left(\frac{d\,n}{d\,x}\right)_s}$$

From the first approximate solution we have

$$n = \sqrt{(r\,\nu/\mathrm{V}\,h)}\ \mathrm{F}(x)$$

Differentiating this and recalling that h is a function of s only leads to

$$\left(\frac{d\,n}{d\,s}\right)_x = -\frac{1}{2}\,\mathrm{F}(x)\sqrt{\left(\frac{r\,\nu}{\mathrm{V}\,h^3}\right)}\,\frac{d\,h}{d\,s}$$

and

$$\left(\frac{d\,n}{d\,x}\right)_s = \mathrm{F}'(x)\sqrt{\left(\frac{r\,\nu}{V\,h}\right)}$$

so that

$$\left(\frac{d\,x}{d\,s}\right)_n = \frac{1}{2\,h}\,\frac{\mathrm{F}(x)}{\mathrm{F}'(x)}\,\frac{d\,h}{d\,s}$$

and the second approximation for $\partial q/\partial s$ is given by

$$\frac{\partial\,q}{\partial\,s} = x\,\frac{d\,v}{d\,s} + \frac{v}{2\,h}\,\frac{\mathrm{F}(x)}{\mathrm{F}'(x)}\,\frac{d\,h}{d\,s}$$

Inserting this value in the original differential equation and proceeding as in the previous solution leads to the result :—

$$\frac{d\,n}{d\,x} = \sqrt{\left(\frac{\nu\,r}{V\,h}\right)} \div \sqrt{\frac{2}{3}\,(x^3 - 3\,x + 2 + \mathrm{M} + \mathrm{N})}$$

$$= (\text{say})\sqrt{\left(\frac{\nu\,r}{V\,h}\right)}\,\mathrm{F'}_2(x)$$

where

$$\mathrm{M} = 3\int_x^{1\cdot0} \varphi(x)\,d\,x: \qquad f(x) = x\,\frac{\mathrm{F}(x)}{\mathrm{F}'(x)}$$

and

$$\mathrm{N} = -\frac{3}{2}\,\frac{\sqrt{(1-p_1)}}{h^2}\,\frac{d\,h}{d\,\theta}\int_x^{1\cdot0} f(x)\,d\,x$$

so that the final result is

$$n = \sqrt{\left(\frac{\nu\,r}{\mathrm{V}h}\right)}\,\mathrm{F}_2(x) \text{ and } \mathrm{F}_2(x)$$

$$= \sqrt{\left(\frac{3}{2}\right)}\int \frac{d\,x}{\sqrt{(x^3 - 3x + 2 + \mathrm{M} + \mathrm{N})}} \qquad (20)$$

Table 6 shows the details of the numerical calculation for various values of θ. The data used is given in Table 5 along with a list of the formulæ used. The values obtained by calculation in Table 6 are compared with the experimental values in fig. 4 (*see also* fig. 3). The differences are generally less than the experimental errors to be expected except perhaps for $\theta = 60°$.

Readings were also taken at $\theta = 50°$ with channel speeds of 22·5 and 5·4 ft./sec. The theoretical values for these speeds are easily deduced from Table 6 by neglecting the small changes inside the integrals due to the slight scale effect on p_1 (*see* fig. 1).

The data used were

for

$$V = 22{\cdot}5, \quad \theta = 50°, \quad v = 31{\cdot}5, \quad \sqrt{(Vh/r\nu)} = 864$$

and for

$$V = 5{\cdot}4, \quad \theta = 50°, \quad v = 7{\cdot}5, \quad \sqrt{(Vh/r\nu)} = 423.$$

From these and the values of $F_2(x)$ in Table 6 for $\theta = 50°$ the values given in Table 6A were easily obtained. The results as shown in fig. 4 again give good agreement with experiment.

Additional experimental evidence in support of the above solution has been obtained by A. Fage at The National Physical Laboratory in connection with an investigation carried out by him on the conditions of flow in the region where the boundary layer separates from the surface.* Mr. Fage's remarks are given in the appendix (*see* page 20).

The intensity of surface friction at any point on the front portion of a cylinder can be estimated by the methods of this paper. Its value is easily found to be

$$f = \mu \frac{dq}{dn} = \rho \frac{\nu^{\frac{1}{2}} V^{1\frac{1}{2}}}{r^{\frac{1}{2}}} \frac{\sqrt{h(1 - p_1)}}{F_2'(x)} \text{ when } n \to 0$$

showing that the skin friction is proportional to $\rho \nu^{\frac{1}{2}} V^{1\frac{1}{2}}$. (c.f. Lanchester's *Aerodynamics* § 36). It is thus possible to estimate the contribution to the drag coefficient made by skin friction. Taking numerical values from theory (Table 6) from $\theta = 0°$ to $\theta = 60°$, and using the experimental curves (fig. 5) to calculate approximate values from $\theta = 60°$ to $\theta = 90°$ the total integrated skin friction drag for the front half of the cylinder was found to be

$$K_D' = 1{\cdot}92 \sqrt{\nu/VD}$$

* The air-flow around a circular cylinder in the region where the boundary layer separates from the surface. R. & M. No. 1179.

The skin friction has become small at 90° and the rear half (90° to 270°) can contribute but little so that probably a close estimate* to the total viscous drag is given by $K_D' = 2 \div \sqrt{VD/\nu}$. This is small compared with the total drag at normal values of Reynold's number but becomes important at low values.

If the thickness δ of the boundary layer is defined as the distance from the surface in which the velocity attains 95 per cent. of the outside velocity, then

$$\delta = c\sqrt{\frac{\nu r}{Vh}} \text{ or } \delta = c\sqrt{\frac{\nu}{d\,v/d\,s}} \quad .. \quad .. \quad (21)$$

where c is the value of F (x) for $x = 0{\cdot}95$ (see Table 6)

(21) can also be written

$$\frac{\delta}{r} = c\sqrt{\frac{2}{h} \cdot \frac{\nu}{VD}}$$

showing that the ratio of the thickness of the boundary layer to the radius of the cylinder is inversely proportional to the square root of Reynolds number.

Conclusion.—It has been shown that the solution obtained for the boundary layer equations holds for the flow over a cylindrical surface throughout the region where the velocity over the surface is increasing. There seems no reason to suppose that it would not hold for any smooth surface provided the same condition was fulfilled (two-dimensional flow being understood). For cylinders other than circular it is probably better to retain dv/ds in the various expressions instead of h. Where the velocity gradient dv/ds becomes small or negative the theory ceases to be valid as this quantity appears under the root sign. In the case of the circular cylinder the change in sign of dv/ds is associated with a complete breakdown of the steady flow.

The experimental velocities in this region are shown in fig. 5. The band which was previously the boundary layer has now become (at $\theta = 90°$) very broad, being in fact the beginning of the eddy region behind the cylinder.

---

* This estimate has since been verified by pressure distribution experiments round small cylinders.

TABLE 2.

Pressure Distribution round Cylinder.

θ	$p_1 = \frac{(p - p_0)}{(p - p_0)\ \text{max.}}$	
	VD = 4·6 ft. ²/sec.	VD = 13·6 ft. ²/sec.
0	1·00	1·00
5	0·98	0·97
10	0·91	0·89
20	0·58	0·60
30	+0·15	+0·13
40	−0·37	−0·44
50	−0·90	−0·96
60	−1·30	−1·45
65	−1·40	
70	−1·46	−1·71
75	−1·42	
80	−1·31	−1·57
85	−1·24	
90	−1·22	−1·41
100	−1·23	−1·30
120	−1·24	−1·11
140	−1·27	−1·07
160	−1·33	−1·05
180	−1·34	−1·02
K_D =	0·64	0·49

TABLE 3.

Total Head near the Surface of a Cylinder in an Air Stream.

V = 12·3 θ = 10° d = 0·4			V = 12·3 θ = 20° d = 0·4			V = 12·3 θ = 30° d = 0·4 — 0·6			V = 12·3 θ = 40° d = 0·4 — 0·6		
n	$H - H_0$	q	n	$H - H_0$	q	n	$H - H_0$	q	n	$H - H_0$	q
0	—0·016	0	0	—0·077	0	0	—0·158	0	0	—0·250	0
0·18	—0·014	1·3	0·18	—0·052	4·6	0·18	—0·082	8·0	0·18	—0·195	6·8
0·26	—0·008	2·6	0·26	—0·042	5·4	0·28	—0·064	8·9	0·28	—0·125	10·3
0·36	—0·005	3·0	0·40	—0·026	6·6	0·38	—0·044	9·8	0·41	—0·079	12·0
0·54	—0·004	3·2	0·54	—0·019	7·0	0·48	—0·036	10·1	0·55	—0·045	13·1
0·73	—0·002	3·4	0·73	—0·012	7·4	0·59	—0·015	11·0	0·84	—0·007	14·3
0·91	—0·002	3·4	0·91	—0·006	7·7	0·76	—0·004	11·4	1·34	+0·002	14·6

V = 12·3 θ = 50° d = 0·4 — 0·6			V = 12·3 θ = 60° d = 0·4 — 0·6			V = 12·3 θ = 60° d = 0·9			V = 12·3 θ = 70° d = 0·4 — 0·6		
n	$H - H_0$	q	n	$H - H_0$	q	n	$H - H_0$	q	n	$H - H_0$	q
0	—0·345	0	0	—0·422	0	0·45	—0·131	15·6	0	—0·438	0
0·18	—0·237	9·5	0·18	—0·322	9·2	0·56	—0·101	16·4	0·18	—0·409	4·9
0·28	—0·177	11·9	0·21	—0·303	10·0	0·67	—0·058	17·5	0·34	—0·323	9·8
0·45	—0·095	14·5	0·28	—0·243	12·1	0·89	—0·023	18·3	0·35	—0·184	14·6
0·61	—0·044	15·9	0·37	—0·022	13·6	1·11	—0·010	18·6	0·91	—0·060	17·8
0·80	—0·009	16·8	0·50	—0·127	15·8	1·33	—0·001	18·8	1·22	—0·014	18·9
1·22	+0·001	17·1	0·75	—0·050	17·7	For comparison			1·44	—0·002	19·2
			1·13	—0·004	18·8	with values by smaller tubes.			2·15	+0·004	19·3

V = 12·3 θ = 80° d = 0·4 — 0·6			V = 12·3 θ = 90° d = 0·58			V = 22·6 θ = 50° d = 0·4			V = 5·4 θ = 50° d = 0·4		
n	$H - H_0$	q	n	$H - H_0$	q	n	$H - H_0$	q	n	$H - H_0$	q
0	—0·424	0	0	—0·405	0	0	—1·20	0	0	—0·064	0
0·18	—0·409	3·6	0·28	—0·395	2·9	0·18	—0·678	21·0	0·18	—0·059	2·1
0·28	—0·403	4·2	0·41	—0·396	2·8	0·28	—0·490	24·4	0·28	—0·050	3·5
0·40	—0·367	6·9	1·10	—0·380	4·6	0·38	—0·273	28·0	0·38	—0·040	4·5
0·90	—0·259	11·8	1·46	—0·313	8·8	0·59	—0·094	30·6	0·55	—0·029	5·4
1·22	—0·144	15·3	1·80	—0·275	10·5	0·79	—0·022	31·5	0·75	—0·015	6·4
1·67	—0·061	17·5	2·4	—0·192	13·4	1·20	0	31·8	0·96	—0·007	6·8
2·10	—0·016	18·5	3·8	—0·021	18·0				1·20	—0·001	7·3
2·55	—0·010	18·7	5·0	+0·005	18·6						
3·2	—0·002	18·8									

V = Channel speed (ft./sec.).
θ = Angle from front generator.
d = External diameter of pitot tube (mm.).
n = Distance of centre of tube from surface (mm.).
$H - H_0$ = Pitot head less head on front generator (lbs./ft.²).
q = Deduced velocity at tube (ft./sec.).

All measurements of head have been corrected for the scale effect shown in Table 1.

TABLE 4.

Mechanical Solution of Boundary Layer Equations for Flow past a Cylinder, Radius = Unity. Channel Velocity = 100 units/sec. Reynolds Number = VD/ν = 28,000

Outside Vel. = v		0	6·35	13·05	19·54	26·02	32·45	38·84	45·2	51·5	57·8	63·9	$k_2 w$ at $\theta = 20°$
$k_2 w$ at $\theta = 0°$	n												
—0·105	0·020	0		13·0		25·9		38·7		51·3		63·7	—0·093
—0·091	0·018		6·49		19·45		32·28		44·96		57·45		—0·080
—0·078	0·016	0		12·9 12·93		25·8 25·80		38·4 38·52		51·0 51·06		63·3 63·38	—0·069
—0·065	0·014		6·41		19·19		31·89		44·41		56·74		—0·058
—0·052	0·012	0		12·6 12·60		25·1 25·14		37·5 37·54		49·7 49·74		61·6 61·72	—0·048
—0·041	0·010		6·08		18·22		30·26		42·14		53·8		—0·037
—0·029	0·008	0		11·3 11·38		22·6 22·68		33·8 33·85		44·8 44·85		55·6 55·63	—0·027
—0·019	0·006		5·00		14·98		24·90		34·64		44·2		—0·017
—0·009..	0·004	0		7·8 7·83		15·6 15·64		23·3 23·28		30·8 30·81		38·3 38·14	—0·008
—0·004	0·002		2·30		6·86		11·39		15·81		20·15		—0·004
0	0	0		0		0		0		0		0	0
$k_2 w$ at	n ↑ / θ →	0	2°	4°	6°	8°	10°	12°	14°	16°	18°	20°	$k_2 w$ at ↑
$\theta = 0$	k_3 →	0	0·35	0·69	1·03	1·36	1·69	2·01	2·32	2·62	2·91	3·18	$\theta = 20°$

TABLE 5.

Summary of Date for Calculating Boundary Layer Velocities.

V = Channel velocity = 12·3 ft./sec.

r = Cylinder Radius = 0·1875 ft.

ν = 0·00016 ft. ^{2}/sec.

θ	p_1	$\frac{dp_1}{d\theta}$	$\sqrt{1-p_1}$	$h=\frac{1}{2\sqrt{1-p_1}}\frac{dp_1}{d\theta}$	$\frac{3}{2}\frac{\sqrt{1-p_1}}{h^2}\frac{dh}{d\theta}$	$\sqrt{\frac{Vh}{r\nu}}$
10	0·89	—1·20	0·32	1·84	—0·045	869
20	0·59	—2·25	0·64	1·75	— 0·38	845
30	+0·13	—2·98	0·93	1·60	— 0·66	810
40	—0·38	—3·10	1·17	1·33	— 1·71	736
50	—0·90	—2·70	1·38	1·00	— 4·35	640
60	—1·30	—1·85	1 52	0·60	— 16·5	496

Explanation of Table 6.

1st approx.

$$F'_1(x) = 1 \div \sqrt{\frac{2}{3}(x^3 - 3x + 2)}$$

$$F_1(x) = \sqrt{2}\log\frac{\sqrt{1-x}\,(\sqrt{3}-\sqrt{2})}{\sqrt{3}-\sqrt{x+2}}$$

2nd approx.

$$\varphi(x) = \frac{1}{F'_1(x)}\int x\,F'_1(x)\,dx \qquad M = 3\int_{x=x}^{x=1}\varphi(x)\,dx$$

$$f(x) = x\,\frac{F_1(x)}{F_1'(x)} \qquad N = -\frac{3}{2}\,\frac{\sqrt{1-p_1}}{h^2}\,\frac{dh}{d\theta}\int_{x=x}^{x=1} f(x)\,dx$$

$$F_2'(x) = 1 \div \sqrt{\frac{2}{3}(x^3 - 3x + 2 + M + N)}$$

$$F_2(x) = \int F_2'(x)\,dx$$

$$n = \sqrt{\frac{\nu r}{V h}}\,F_2(x) \qquad q = xv \qquad v = V\sqrt{1-p_1}$$

TABLE 6A.

Calculated Values for Channel Speeds of 22·5 and 5·4 ft./sec.

$\theta = 50°$

V	x =	0	0·1	0·2	0·3	0·4	0·5	0·6	0·7	0·8	0·9	0·95
22·5	n (mm.)	0	0·026	0·054	0·083	0·115	0·151	0·192	0·240	0·303	0·405	0·495
	q (ft./sec)	0	3·2	6·3	9·5	12·7	15·9	19·0	22·2	25·4	28·5	30·1
5·4	n (mm.)	0	0·053	0·11	0·17	0·24	0·31	0·39	0·49	0·62	0·83	1·01
	q (ft./sec.)	0	0·75	1·50	2·25	3·0	3·75	4·5	5·2	6·0	6·7	7·1

TABLE 6.

Calculation of Boundary Layer Velocities for V = 12·3 *ft./sec.*

θ	$x =$		0	0·1	0·2	0·3	0·4	0·5	0·6	0·7	0·8	0·9	0·95
All values.	$F'_1(x)$	=	0·866	0·939	1·032	1·154	1·316	1·55	1·90	2·48	3·66	7·18	14·23
	$F_1(x)$	=	0	0·088	0·188	0·296	0·420	0·565	1·735	0·952	1·250	1·75	2·25
	$\int x F'(x)\,dx$	=	0	0·0045	0·0192	0·046	0·090	0·155	0·248	0·390	0·613	1·04	1·51
	$\varphi(x)$	=	0	0·005	0·019	0·040	0·072	0·100	0·143	0·157	0·193	0·173	0·128
	M	=	0·26	0·26	0·26	0·25	0·24	0·213	0·174	0·078	0·021	0·101	0·001
	$f(x)$	=	0	0·0094	0·036	0·077	0·128	0·182	0·232	0·269	0·273	0·219	0·150
	$\int_x^{1·0} f(x)\,dx$	=	0·145	0·144	0·142	0·136	0·126	0·111	0·090	0·065	0·038	0·013	0·004
	$x^3 - 3x + 2$	=	2·00	1·701	1·408	1·120	0·864	0·626	0·416	0·244	0·112	0·029	0·001
10°	N	=	0·007	0·007	0·006	0·006	0·006	0·005	0·004	0·003	0·002	0·001	0
	$x^3 - 3x + 2 + M + N$	=	2·26	1·97	1·68	1·39	1·16	0·844	0·594	0·376	0·192	0·051	0·017
	$F_2'(x)$	=	0·81	0·87	0·95	1·04	1·14	1·33	1·59	2·00	2·80	5·4	9·4
	$F_2(x)$	=	0	0·084	0·175	0·274	0·383	0·51	0·65	0·83	1·07	1·48	1·84
	n (mm.)	=	0	0·03	0·06	0·10	0·14	0·18	0·23	0·29	0·38	0·52	0·66
	q (ft./sec)	=	0	0·4	0·8	1·2	1·6	2·0	2·4	2·8	3·2	3·6	3·8
20°	N	=	0·06	0·05	0·05	0·05	0·05	0·04	0·03	0·02	0·014	0·005	0·001
	$x^3 - 3x + 2 + M + N$	=	2·32	2·01	1·72	1·43	1·15	0·88	0·62	0·39	0·204	0·055	0·018
	$F'_2(x)$	=	0·81	0·86	0·94	1·03	1·14	1·31	1·56	1·97	2·71	5·2	9·1
	$F_2(x)$	=	0	0·083	0·17	0·27	0·38	0·50	0·64	0·82	1·05	1·44	1·79
	n (mm.)	=	0	0·03	0·06	0·10	0·14	0·18	0·23	0·30	0·38	0·52	0·65
	q (ft./sec.)	=	0	0·8	1·6	2·4	3·1	3·9	4·7	5·5	6·3	7·1	7·5
30°	N	=	0·09	0·09	0·09	0·09	0·08	0·07	0·06	0·04	0·02	0·01	0
	$x^3 - 3x + 2 + M + N$	=	2·35	2·05	1·76	1·47	1·18	0·91	0·65	0·41	0·21	0·06	0·017
	$F'_2(x)$	=	0·80	0·85	0·92	1·01	1·13	1·29	1·52	1·91	2·68	5·0	9·4
	$F_2(x)$	=	0	0·082	0·17	0·27	0·37	0·50	0·64	0·81	1·04	1·41	1·78
	n (mm.)	=	0	0·03	0·06	0·10	0·14	0·19	0·24	0·30	0·39	0·53	0·67
	q (ft./sec.)	=	0	1·2	2·3	3·5	4·6	5·8	6·9	8·1	9·2	10·4	10·9

40°	N	=	0·25	0·25	0·24	0·23	0·22	0·19	0·15	0·11	0·065	0·022	0·007
	$x^3 - 3x + 2 + M + N$	=	2·51	2·21	1·91	1·61	1·32	1·03	0·74	0·48	0·255	0·072	0·024
	$F'_2(x)$	=	0·77	0·82	0·89	0·97	1·07	1·21	1·43	1·77	2·44	4·6	7·9
	$F_2(x)$	=	0	0·080	0·165	0·268	0·370	0·48	0·616	0·776	0·99	0·34	1·65
	n (mm.)	=	0	0·03	0·07	0·11	0·15	0·20	0·25	0·32	0·41	0·55	0·68
	q (ft./Sec.)	=	0	1·4	2·9	4·3	5·8	7·2	8·6	10·1	11·5	13·0	13·7
50°	N	=	0·63	0·63	0·62	0·59	0·55	0·482	0·392	0·283	0·165	0·058	0·018
	$x^3 - 3x + 2 + M + N$	=	2·89	2·59	2·29	1·97	1·65	1·32	0·982	0·656	0·355	0·108	0·035
	$F'_2(x)$	=	0·72	0·76	0·81	0·88	0·95	1·06	1·24	1·51	2·06	3·72	6·54
	$F_2(x)$	=	0	0·074	0·152	0·236	0·328	0·429	0·544	0·681	0·86	1·15	1·40
	n (mm.)	=	0	0·035	0·072	0·112	0·156	0·204	0·259	0·32	0·41	0·56	0·67
	q (ft./sec.)	=	0	1·7	3·4	5·1	6·8	8·5	10·2	11·9	13·6	15·3	16·1
60°	N	=	2·40	2·39	2·34	2·25	2·08	1·82	1·49	1·07	0·626	0·219	0·066
	$x^3 - 3x + 2 + M + N$	=	4·66	4·35	4·01	3·62	3·18	2·66	2·08	1·44	0·816	0·269	0·083
	$F'_2(x)$	=	0·57	0·59	0·61	0·64	0·69	0·75	0·85	1·02	1·36	2·37	4·25
	$F_2(x)$	=	0	0·058	0·118	0·181	0·247	0·319	0·399	0·493	0·611	0·798	0·964
	n (mm).	=	0	0·036	0·072	0·111	0·152	0·196	0·245	0·303	0·376	0·490	0·593
	q (ft./sec.)	=	0	1·87	3·74	5·6	7·5	9·4	11·2	13·1	15·0	16·8	17·8

Appendix.

A NOTE ON THE PRECEDING PAPER

By A. Fage, A.R.C.S.

September, 1928.

The purpose of the present note is to show that further experimental evidence in support of Dr. Thom's solution can be obtained from observations taken in the investigation, recently undertaken by the writer, on the conditions of flow in the region where the boundary layer separates from the surface (R. & M. 1179). This investigation was made on a cylinder of large diameter (8·9 inches) and covered a range of wind speed from 22·0 to 71·4 feet per second, over which the drag coefficient drops from 0·60 to 0·20 approximately, and the character of the flow undergoes a marked change. Although attention was mainly focussed on the conditions of flow near the "breakaway" region, observations of total head were also taken across several sections of the boundary layer forward of this region, and where Dr. Thom's solution is applicable. Values of the velocity (q) at points in these sections, expressed as a fraction of the maximum velocity (v) at the outer limit of the layer, and estimated as in R. & M. 1179, from the observations of total head taken at the extreme speeds 22·0 and 71·4 feet per second are given in figs. 6 and 7. It will be observed in each of these figures that (as mentioned in R. & M. 1179) the character of the velocity distribution is practically independent of the position of the section, for the range of θ chosen. Included in figs. 6 and 7 are curves showing, for the chosen sections, the distributions of velocity estimated from Dr. Thom's solution. It is seen that, provided the section is not taken near the point of maximum velocity on the cylinder, the points representing the experimental observations lie very closely on the appropriate theoretical curves. The comparison supports, therefore, Dr. Thom's conclusions, that his solution of the boundary layer equations holds for the flow over a cylindrical surface, except in the region where the velocity gradient around the cylinder tends to a small or negative value.

R.&M.1176.

FIG.1.

THE BOUNDARY LAYER ON THE FRONT PORTION OF A CYLINDER.

Pressure distribution round stationary cylinder.

Cylinder diameter = 4·5 inches.

—●— Wind speed = 12·3 ft/sec.

--×-- " " = 36 ft/sec.

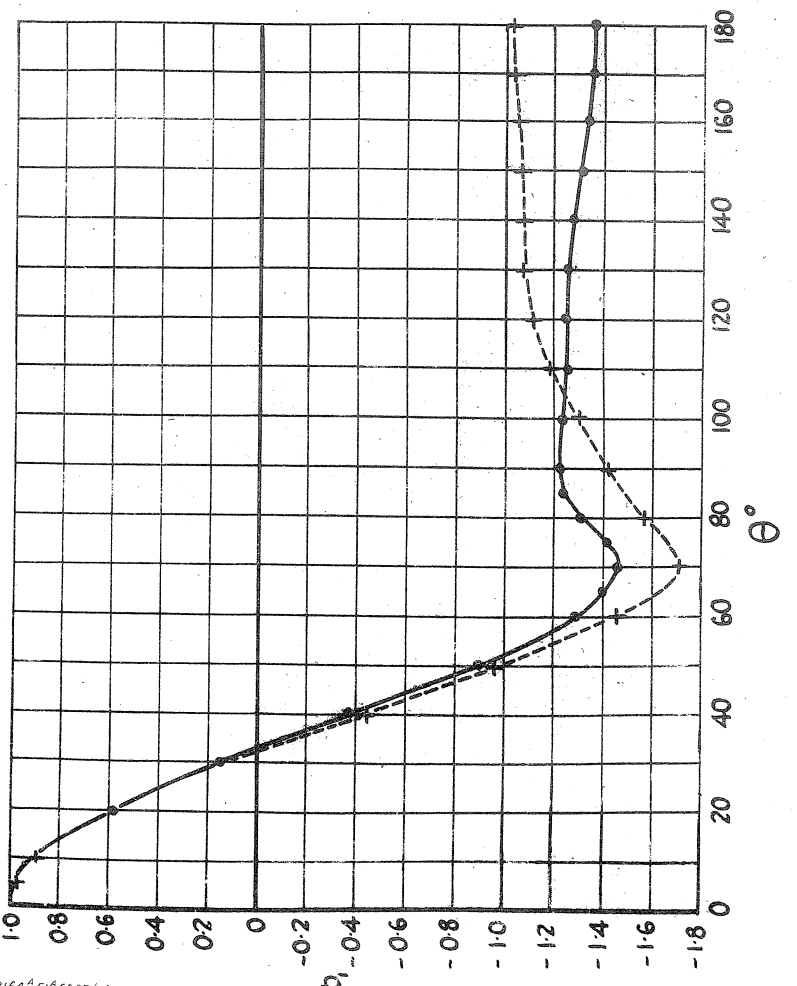

P.2164 A.51 A 6007/1607 775.1/29.

Malloy & Son, Photo-Lith.

FIG. 2.

THE BOUNDARY LAYER ON THE FRONT PORTION OF A CYLINDER.

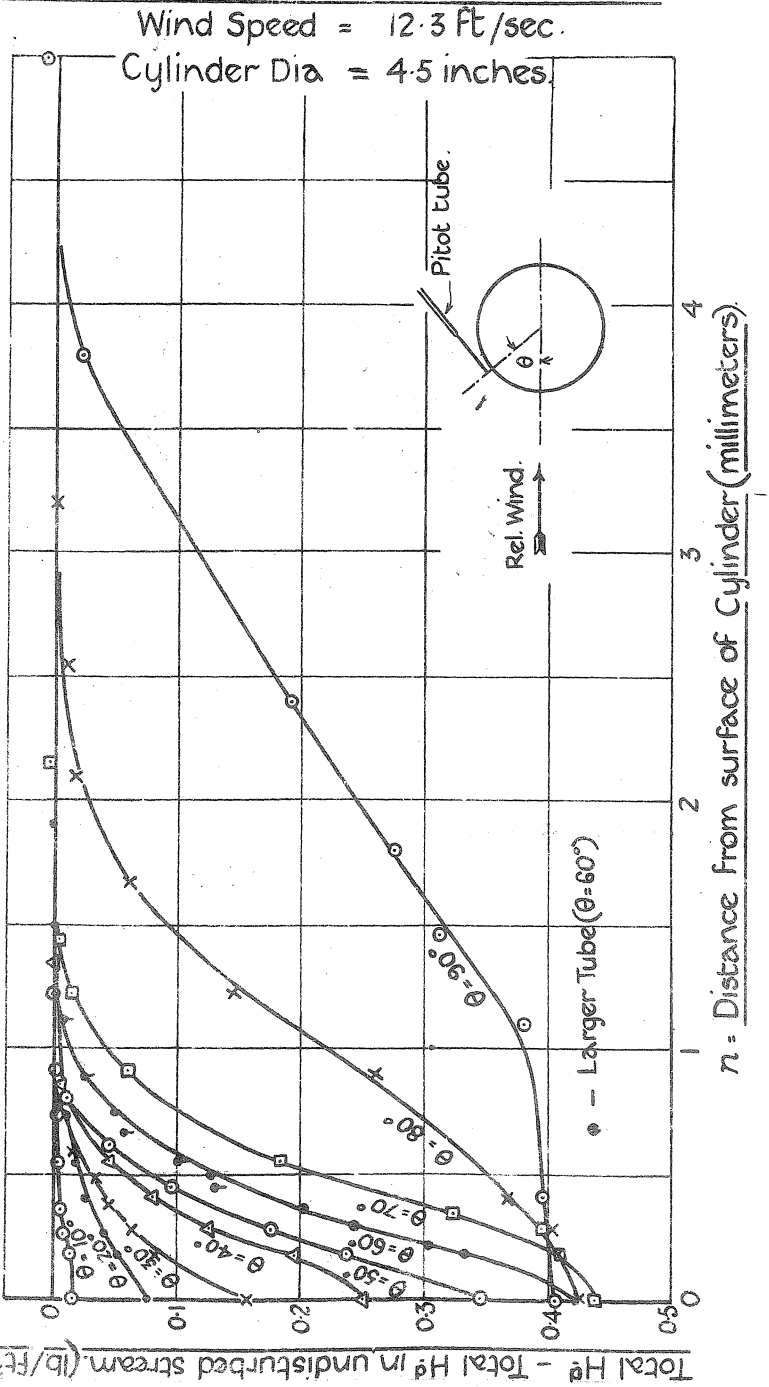

R. & M. 1176.

THE BOUNDARY LAYER ON THE FRONT PORTION OF A CYLINDER.

FIG. 3.

Comparison of various solutions and experiments.

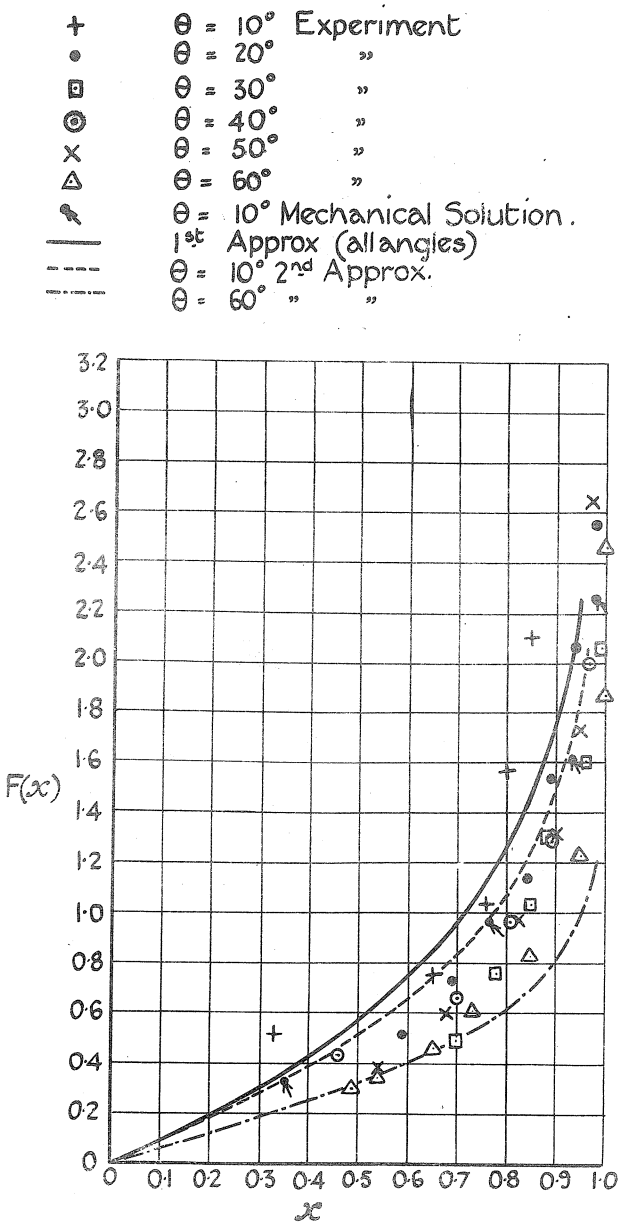

R.&M.1176.

THE BOUNDARY LAYER ON THE FRONT PORTION OF A CYLINDER.

FIG. 4.

Comparison of observed and calculated velocities.

⊙ Experimental value. —⊙— Calculated values.

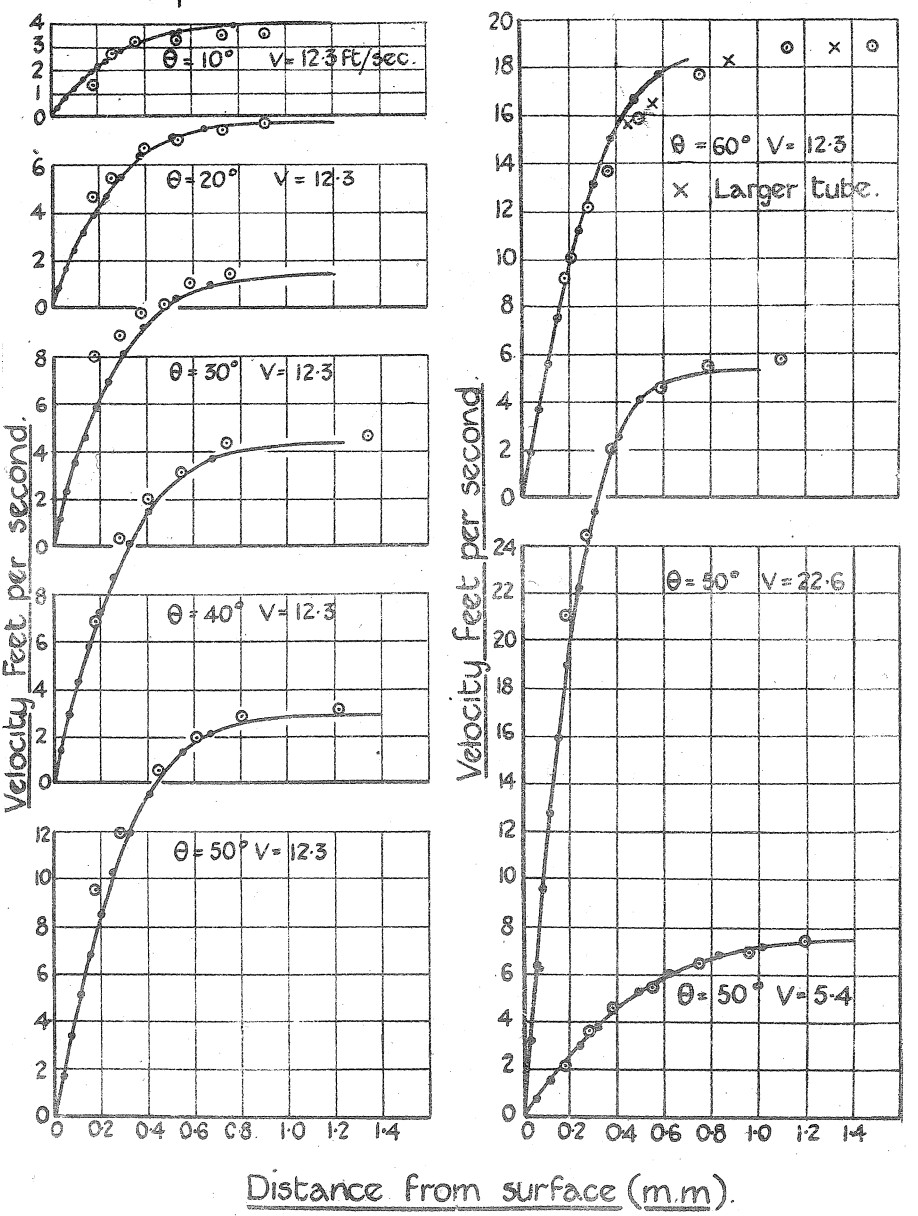

R. & M. 1176.

FIG. 5.

THE BOUNDARY LAYER ON THE FRONT PORTION OF A CYLINDER.

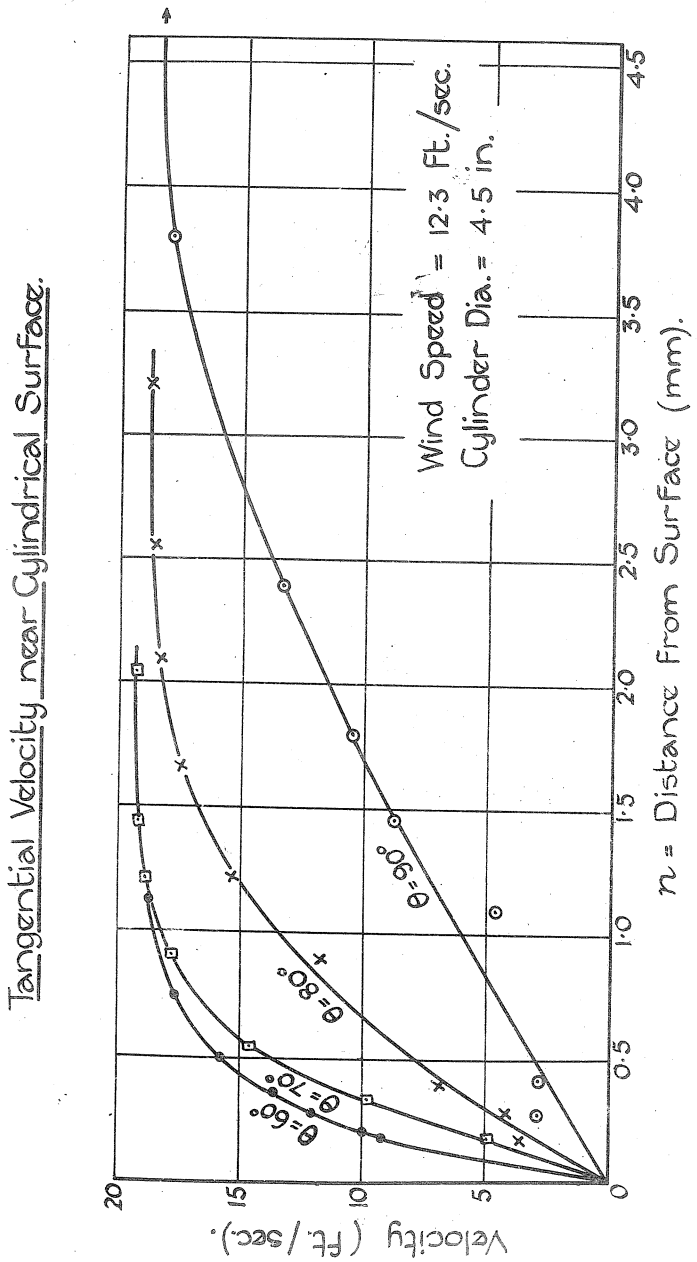

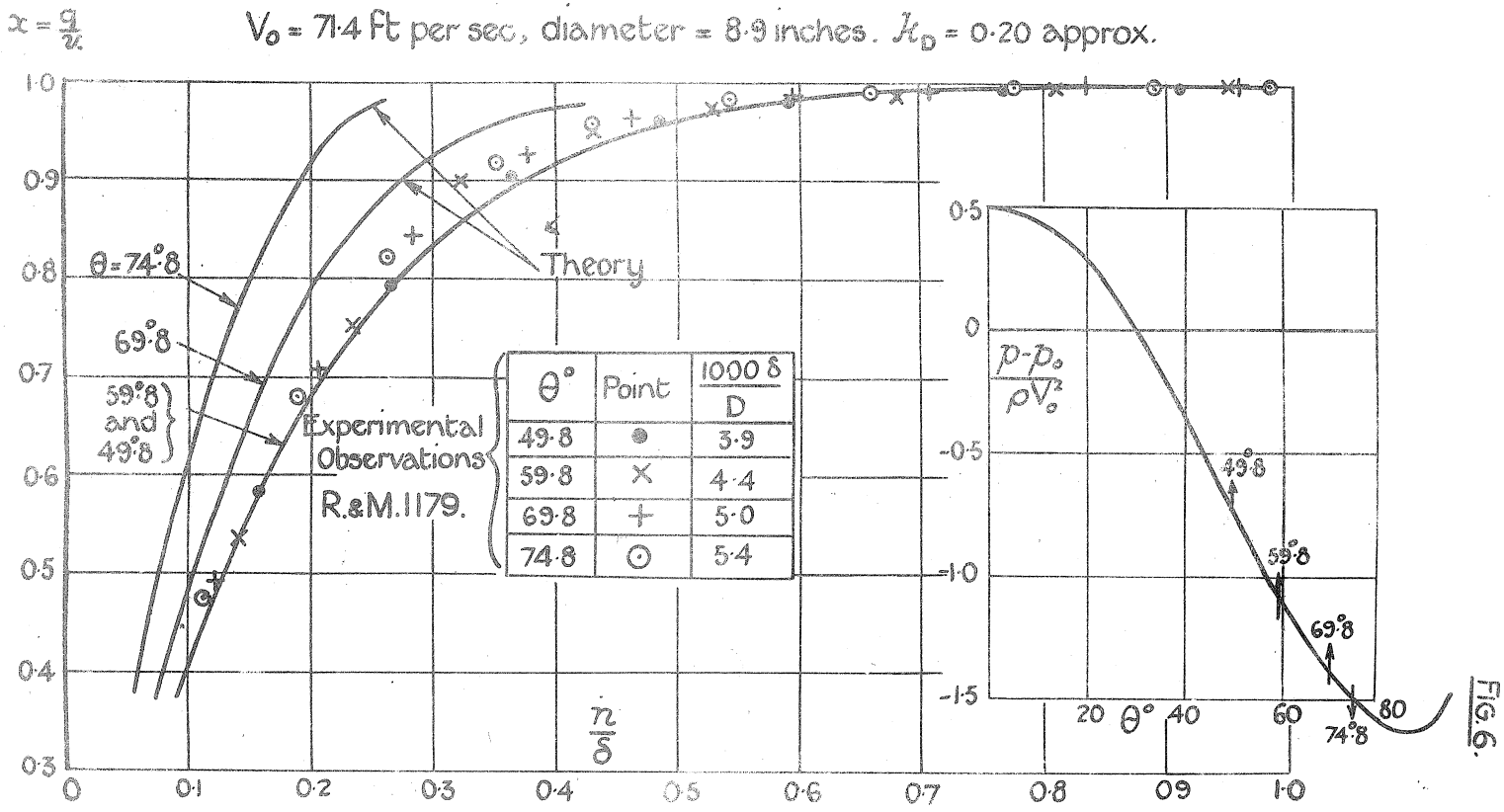
$x = \frac{q}{u}$
V_0 = 71·4 ft per sec, diameter = 8·9 inches. k_D = 0·20 approx.
1·0
0·9
0·8
0·7
0·6
0·5
0·4
0·3
0
0·1
0·2
0·3
0·4
0·5
0·6
0·7
0·8
0·9
1·0
$\frac{n}{\delta}$
θ = 74°8
69°8
59°8 and 49°8
Theory
Experimental Observations R.&M.1179.
θ° | Point | 1000 δ / D
49·8 | ● | 3·9
59·8 | × | 4·4
69·8 | + | 5·0
74·8 | ⊙ | 5·4
0·5
0
-0·5
-1·0
-1·5
$\frac{p-p_0}{\rho V_0^2}$
49°8
59°8
69°8
74°8
20
θ°
40
60
80

FIG. 6.

V_0 = 22·0 ft per sec, diameter = 8·9 inches. $\mathcal{R}_D$ = 0·60 approx.

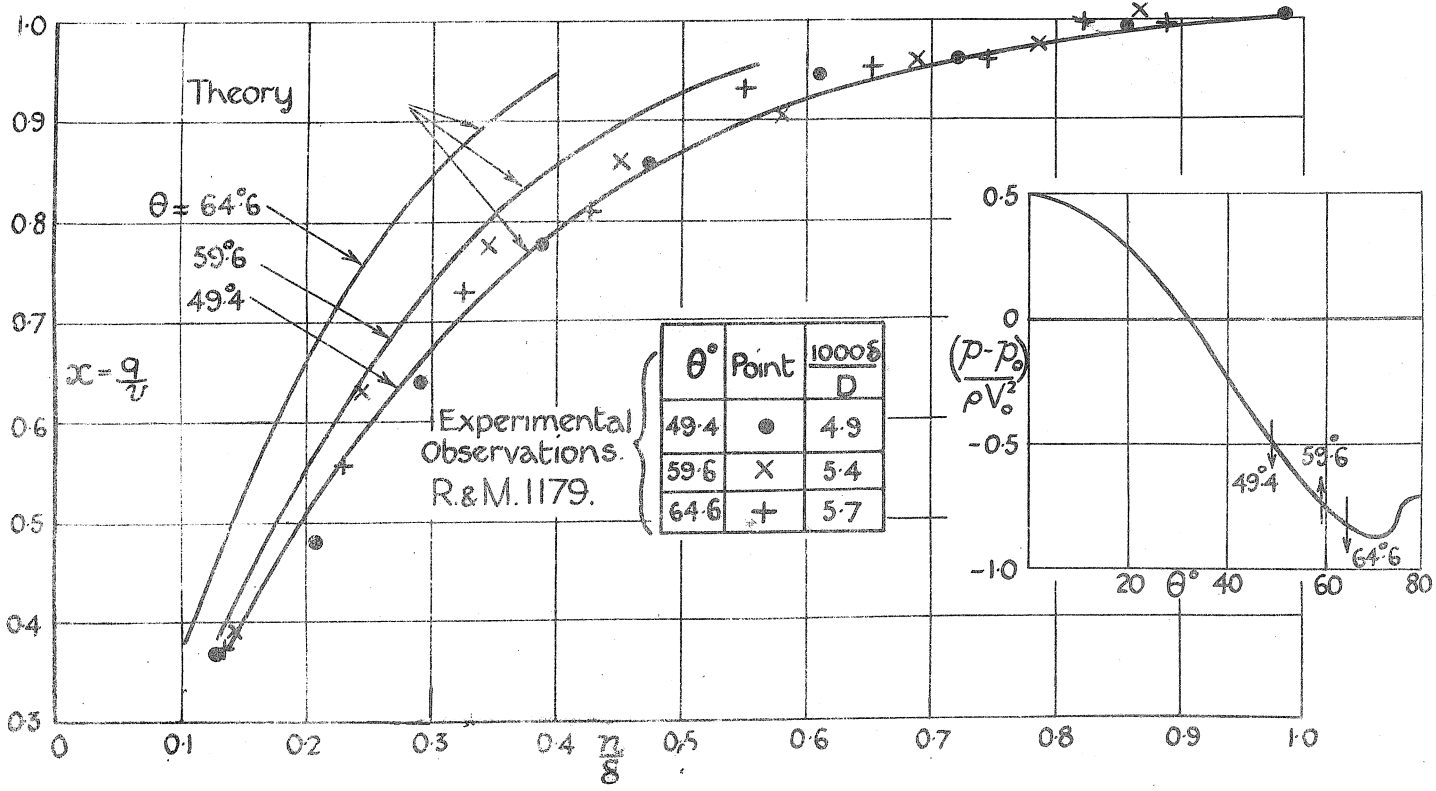

FIG. 7.

SYSTEM OF AXES.

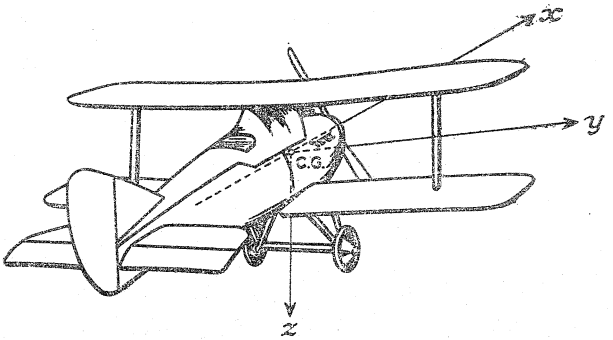

Axes	Symbol Designation. Positive direction	x longitudinal forward	y lateral starboard	z normal downward
Force	Symbol	X	Y	Z
Moment	Symbol Designation	L rolling	M pitching	N yawing
Angle of Rotation	Symbol	ϕ	θ	ψ
Velocity	Linear Angular	u p	v q	w r
Moment of Inertia		A	B	C

Components of linear velocity and force are positive in the positive direction of the corresponding axis. Components of angular velocity and moment are positive in the cyclic order y to z about the axis of x, z to x about the axis of y, and x to y about the axis of z.

The angular movement of a control surface (elevator or rudder) is governed by the same convention, the elevator angle being positive downwards and the rudder angle positive to port. The aileron angle is positive when the starboard aileron is down and the port aileron is up. A positive control angle normally gives rise to a negative moment about the corresponding axis. The symbols for the control angles are :–

ξ aileron angle
η elevator angle
η_T tail setting angle
ζ rudder angle

Recent Publications of the

AERONAUTICAL RESEARCH COMMITTEE

The publications named below can be purchased at the net prices shown (postage extra) from H.M. Stationery Office at the addresses shown on page 1 of cover, or through any bookseller :—

	s.	d.
TECHNICAL REPORT of the Aeronautical Research Committee for the year 1924–25, with Appendices—		
Vol. I. Aeroplanes, Model and Full Scale - -	17	6
Vol. II. Airscrews, Engines, Materials, etc. - -	17	6
TECHNICAL REPORT of the Aeronautical Research Committee for the year 1925–26 - - - -	35	0
REPORT of the Aeronautical Research Committee for the year 1925–26 - - - - - - - -	2	0
REPORT of the Aeronautical Research Committee for the year 1926–27 - - - - - - - -	2	0

Reports & Memoranda. *LIST OF PUBLICATIONS.*

No. 650.	Reports and Memoranda of the Advisory Committee published on or before 31st March, 1920 - -	9*d.*
„ 750.	Reports and Memoranda of the Aeronautical Research Committee published between 1st April, 1920 and 30th September, 1921 - - - - -	2*d.*
„ 850.	Reports and Memoranda of the Aeronautical Research Committee published between 1st October, 1921 and 31st March, 1923 - - - - -	1*d.*
„ 950.	Reports and Memoranda of the Aeronautical Research Committee published between 1st April, 1923 and 31st December, 1924 - - - - -	4*d.*
„ 1050.	Reports and Memoranda of the Aeronautical Research Committee published between 1st January, 1925 and 28th February, 1927 - - - - -	4*d.*
„ 1150.	Reports and Memoranda of the Aeronautical Research Committee published between 1st March, 1927 and 30th June, 1928 - - - - - - -	4*d.*

*LIST OF PUBLICATIONS ON AERONAUTICS.**

List B. Revised to 1st April, 1927.

B.1. Air Ministry Publications.

B.2. Aeronautical Research Committee Publications.

* This list may be obtained on application to H.M. Stationery Office.